



Design, synthesis, biophysical and biological studies of trisubstituted naphthalimides as G-quadruplex ligands

Antonella Peduto^{a,†}, Bruno Pagano^{a,†}, Carmen Petronzi^a, Antonio Massa^b, Veronica Esposito^c, Antonella Virgilio^c, Francesco Paduano^d, Francesco Trapasso^d, Filomena Fiorito^e, Salvatore Florio^f, Concetta Giancola^g, Aldo Galeone^{c,*}, Rosanna Filosa^{a,*}

^a Dipartimento di Scienze Farmaceutiche e Biomediche, Università di Salerno, Via Ponte don Melillo, 84084 Fisciano (SA), Italy

^b Dipartimento di Chimica, Università di Salerno, Via Ponte don Melillo, 84084 Fisciano (SA), Italy

^c Dipartimento di Chimica delle Sostanze Naturali, Università degli Studi di Napoli Federico II, Via D. Montesano, 49 80131 Napoli, Italy

^d Dipartimento di Medicina Sperimentale e Clinica, Università Magna Grecia di Catanzaro, Viale Europa, 88100 Catanzaro, Italy

^e Dipartimento di Patologia e Sanità Animale, Università degli Studi di Napoli Federico II, Via Delpino 1, 80137 Napoli, Italy

^f Dipartimento di Strutture, Funzioni e Tecnologie Biologiche, Università degli Studi di Napoli Federico II, Via Delpino 1, 80137 Napoli, Italy

^g Dipartimento di Chimica 'P. Corradini', Università degli Studi di Napoli Federico II, Via Cintia, 80126 Napoli, Italy

ARTICLE INFO

Article history:

Received 3 April 2011

Revised 28 July 2011

Accepted 28 August 2011

Available online 1 September 2011

Keywords:

Naphthalimides

G-Quadruplex

Telomerase

Cancer

ABSTRACT

A series of trisubstituted naphthalimides have been synthesized and evaluated as telomeric G-quadruplex ligands by biophysical methods. Affinity for telomeric G-quadruplex AGGG(TTAGGG)₃ binding was first screened by fluorescence titrations. Subsequently, the interaction of the telomeric G-quadruplex with compounds showing the best affinity has been studied by isothermal titration calorimetry and UV-melting experiments. The two best compounds of the series tightly bind the telomeric quadruplex with a 2:1 drug/DNA stoichiometry. These derivatives have been further evaluated for their ability to inhibit telomerase by a TRAP assay and their pharmacological properties by treating melanoma (M14) and human lung cancer (A549) cell lines with increasing drug concentrations. A dose-dependent inhibition of cell proliferation was observed for all cellular lines during short-term treatment.

© 2011 Elsevier Ltd. All rights reserved.

1. Introduction

G-Quadruplexes are unique DNA secondary structures based on the building block called G-quartet (also known as G-tetrad). This substructure is formed by the association of four guanines into a cyclic arrangement in which the bases are held together by eight Hoogsteen hydrogen bonds. Several G-quartets can stack each other to generate a range of structures (monomolecular, bimolecular and tetramolecular) exhibiting an extensive structural diversity and polymorphism compared to duplex DNA. Recent researches suggest that human genome could contain over 300,000 sequences potentially able to form G-quadruplexes¹ and a number of relevant regions has been reported to adopt these structures including several oncogene promoter regions, telomeric ends, ribosomal DNA, mini-satellites and the immunoglobulin heavy chain switch region. For these reasons, the G-quadruplex structures adopted by these sequences can be regarded as potential new pharmacological targets.² Among these, telomeric G-quadruplexes represent particularly appealing targets and they have been the topic of several

researches.³ The key function of telomeres is to protect chromosomal termini from exonucleases and ligases, thus preventing degradation or end-fusion and maintaining stability.^{4,5} Several intramolecular G-quadruplex structures formed by the human telomeric repetitive DNA sequence (TTAGGG)_n have been described, depending on the conditions and technique employed.^{6–9} Potassium-stabilized G-quadruplex structures formed by the telomere substrate inhibit in vitro telomere maintenance by the enzyme telomerase.¹⁰ Since elevated telomerase activity has been implicated in ~85% of cancers,¹¹ its inhibition represents an attractive strategy for the development of selective anticancer drugs.^{12,13} In fact, G-quadruplex-interactive inhibitors of telomerase may offer a less challenging developmental pathway to the clinic than antisense agents targeted directly against components of the telomerase ribonucleoprotein complex.^{14,15} The formation and stabilization of G-quadruplex structures at the telomeric ends have been reported to impede the telomerase association and to increase the genomic instability by hampering the recognition of telomere-associated proteins with their targets.^{16,17} Although G-quadruplex structures can be targeted by several types of organic small ligands through various binding modes, the development of most of small molecules as G-quadruplex binders has been largely based on polycyclic planar aromatic compounds with at least

* Corresponding authors.

E-mail addresses: galeone@unina.it (A. Galeone), rfilosa@unisa.it (R. Filosa).

† These authors contributed equally to this work.

one substituent, usually two, terminating in a cationic group.^{18,19} The rationale for the planar moiety has been that this would stack effectively onto planar G-quartets, which has been confirmed by several crystallographic and NMR studies of G-quadruplex–ligand complexes.^{20–25} Different structures with these characteristics have been identified with high affinity and selectivity for the human telomeric quadruplex.²⁶ However, there is still a growing interest in the design and screening of newer chemical structures as potential G-quadruplex ligands, with the aim of developing more potent and selective molecules. Recently, tri-, tetra- and heptacyclic perylene analogues as DNA telomerase inhibitors have been reported.²⁷ Among these, the monosubstituted naphthalimides showed poor telomerase inhibition properties. However, the potential of naphthalimido derivatives as effective G-quadruplex ligands and their possible therapeutic properties have not exhaustively investigated. In the present paper, we describe the design and the synthesis of several trisubstituted naphthalimides and their ability to interact with a telomeric quadruplex, namely AGGG(TTAGGG)₃.⁹ The evaluation of the capacity of these compounds to inhibit telomerase and their activity against human cancer cells are reported, as well.

2. Materials and methods

2.1. Chemistry

All reagents were analytical grade and purchased from Sigma–Aldrich (Milano, Italy). Flash chromatography was performed on Carlo Erba Silica Gel 60 (230–400 mesh; Carlo Erba, Milano, Italy). TLC was carried out using plates coated with Silica Gel 60F 254 nm purchased from Merck (Darmstadt, Germany). ¹H and ¹³C NMR spectra were registered on a Bruker AC 300. Chemical shifts are reported in ppm. The abbreviations used are as follows: s, singlet; d, doublet; dd double doublet; br, broad signal. MS spectrometry analysis ESI-MS was carried out on a Finnigan LCQ Deca ion trap instrument. Elemental analysis was performed by Desert Analytics (Tucson, AZ). Melting points were determined in open capillary tubes on an Electrothermal 9100 apparatus and are uncorrected.

2.1.1. 3,6-Diamino-1,8-naphthalic anhydride (3)

To a solution of 3,6-dinitro-1,8-naphthalic anhydride²⁸ (7.42 g, 25.7 mmol) in 188 mL of DMF/MeOH (4:1) ammonium formate (15.07 g, 0.231 mol) and 10% palladium charcoal (0.151 g, 1.42 mmol) were added. The mixture was stirred for 2 h at room temperature. The solid was filtered off and the filtrate was concentrated on a rotary evaporator. To the resulting concentrate, containing DMF, cold water was added. The precipitate was filtered and crystallized from DMF/H₂O to give 3,6-diamino-1,8-naphthalic anhydride as a yellow powder (5.21 g, 89%). ¹H NMR (DMSO-*d*₆) 5.79 (s, 2NH₂); 6.97 (d, 2H, *J* = 2.19 Hz); 7.53 (d, 2H, *J* = 2.19 Hz).

2.1.2. General procedures for 4–13

To a suspension of compound **3** (0.200 g, 0.87 mmol) in toluene (5 mL), a solution of desired amine (3 equiv) dissolved in 3 mL of EtOH was added. The reaction was refluxed for 3 h. The mixture was allowed to cool to room temperature.

2.1.2.1. 5,8-Diamino-2-(2-(dimethylamino)ethyl)-1H-benzo[de]isoquinoline-1,3(2H)-dione (4)

Compound **4** was obtained by precipitation from reaction mixture (yield: 67%). ¹H NMR (DMSO-*d*₆): 2.22 (s, 6H); 2.52 (t, 2H, *J* = 7.23 Hz); 4.11 (t, 2H, *J* = 7.23 Hz); 5.65 (s, 2NH₂); 6.98 (d, 2H, *J* = 2.19 Hz); 7.56 (d, 2H, *J* = 2.19 Hz).

2.1.2.2. 5,8-Diamino-2-(2-(pyrrolidin-1-yl)ethyl)-1H-benzo[de]isoquinoline-1,3(2H)-dione (5)

Compound **5** was obtained by precipitation from reaction mixture (yield: 93%). ¹H NMR (CDCl₃) 1.90 (br, 4H); 2.73 (br, 4H); 2.98 (t, 2H, *J* = 7.45 Hz); 4.15 (s, 2NH₂); 4.41 (t, 2H, *J* = 7.45 Hz); 7.15 (d, 2H, *J* = 2.19 Hz); 7.86 (d, 2H, *J* = 2.19 Hz).

2.1.2.3. 5,8-Diamino-2-(2-(piperidin-1-yl)ethyl)-1H-benzo[de]isoquinoline-1,3(2H)-dione (6)

Solvent was evaporated and the residue was chromatographed on silica gel eluting with CHCl₃/MeOH/NH₄OH 9.5/0.15/0.25 to give **6** (63%). ¹H NMR (CDCl₃) 1.52 (br, 6H); 2.52 (br, 4H); 2.73 (t, 2H, *J* = 7.45 Hz); 4.12 (s, 2NH₂); 4.39 (t, 2H, *J* = 7.45 Hz); 7.12 (d, 2H, *J* = 2.19 Hz); 7.88 (d, 2H, *J* = 2.19 Hz).

2.1.2.4. 5,8-Diamino-2-(2-morpholinoethyl)-1H-benzo[de]isoquinoline-1,3(2H)-dione (7)

Solvent was evaporated and the residue was chromatographed on silica gel eluting with CHCl₃/MeOH/NH₄OH 9.5/0.15/0.25 to give **7** (60%). ¹H NMR (DMSO-*d*₆) 2.52 (br, 6H); 3.53 (t, 4H, *J* = 5.92 Hz); 4.16 (t, 2H, *J* = 7.45 Hz); 5.85 (s, 2NH₂); 6.98 (d, 2H, *J* = 2.19 Hz); 7.56 (d, 2H, *J* = 2.19 Hz).

2.1.2.5. 5,8-Diamino-2-(3-(piperazin-1-yl)ethyl)-1H-benzo[de]isoquinoline-1,3(2H)-dione (8)

Compound **8** was obtained by precipitation from reaction mixture (yield: 75%). ¹H NMR (CD₃OD) 2.52 (br, 4H); 2.92 (br, 6H); 4.26 (t, 2H, *J* = 7.45 Hz); 7.12 (d, 2H, *J* = 2.19 Hz); 7.76 (d, 2H, *J* = 2.19 Hz).

2.1.2.6. 5,8-Diamino-2-(3-(dimethylamino)propyl)-1H-benzo[de]isoquinoline-1,3(2H)-dione (9)

Solvent was evaporated and the residue was chromatographed on silica gel eluting with CHCl₃/MeOH/NH₄OH 9.5/0.15/0.25 to give **9** (63%). ¹H NMR (CDCl₃) 1.82–1.93 (m, 2H); 2.24 (s, 6H); 2.47 (t, 2H, *J* = 7.23 Hz); 4.00 (2NH₂); 4.19 (t, 2H, *J* = 7.23 Hz); 7.02 (d, 2H, *J* = 2.19 Hz); 7.76 (d, 2H, *J* = 2.19 Hz).

2.1.2.7. 5,8-Diamino-2-(3-(pyrrolidin-1-yl)propyl)-1H-benzo[de]isoquinoline-1,3(2H)-dione (10)

Solvent was evaporated and the residue was chromatographed on silica gel eluting with CHCl₃/MeOH/ NH₄OH 9/1/0.5 to give **10** (65%). ¹H NMR (CDCl₃) 1.88 (br, 4H); 2.00 (m, 2H); 2.57 (br, 4H); 2.66 (t, 2H, *J* = 7.45 Hz); 4.15 (s, 2NH₂); 4.24 (t, 2H, *J* = 7.45 Hz); 7.15 (d, 2H, *J* = 2.19 Hz); 7.78 (d, 2H, *J* = 2.19 Hz).

2.1.2.8. 5,8-Diamino-2-(3-(piperidin-1-yl)propyl)-1H-benzo[de]isoquinoline-1,3(2H)-dione (11)

Solvent was evaporated and the residue was chromatographed on silica gel eluting with CHCl₃/MeOH/NH₄OH 9.5/0.15/0.25 to give **11** (62%). ¹H NMR (CDCl₃) 1.52 (br, 6H); 1.98 (m, 2H); 2.47 (br, 4H); 2.51 (t, 2H, *J* = 7.45 Hz); 4.00 (s, 2NH₂); 4.21 (t, 2H, *J* = 7.45 Hz); 7.10 (d, 2H, *J* = 2.19 Hz); 7.78 (d, 2H, *J* = 2.19 Hz).

2.1.2.9. 5,8-Diamino-2-(3-morpholinopropyl)-1H-benzo[de]isoquinoline-1,3(2H)-dione (12)

Solvent was evaporated and the residue was chromatographed on silica gel eluting with CHCl₃/MeOH/NH₄OH 9.5/0.15/0.25 to give **12** (63%). ¹H NMR (CDCl₃) 1.88 (m, 2H); 2.48 (br, 4H); 2.50 (t, 2H, *J* = 7.45 Hz); 3.53 (t, 4H, *J* = 5.92 Hz); 3.98 (s, 2NH₂); 4.12 (t, 2H, *J* = 7.45 Hz); 6.98 (d, 2H, *J* = 2.19 Hz); 7.62 (d, 2H, *J* = 2.19 Hz).

2.1.2.10. tert-Butyl-4-(3-(5,8-diamino-1,3-dioxo-1H-benzo[de]isoquinolin-2(3H)-yl)propyl)piperazine-1-carboxylate (13)

Solvent was evaporated and the residue was chromatographed on silica gel eluting with CHCl₃/MeOH/NH₄OH 9.5/0.25/0.15 to give

13 (80%). ¹H NMR (CDCl₃) 1.56 (s, 9H); 1.93 (br, 2H); 2.42 (br, 4H); 2.53 (t, 2H, *J* = 7.2 Hz); 3.33 (br, 4H); 4.02 (s, 2H); 4.21 (t, 2H, *J* = 7.2 Hz); 7.12 (d, 2H, *J* = 2.19 Hz); 7.76 (d, 2H, *J* = 2.19 Hz).

2.1.3. General procedures for 14–23

A solution of compounds **4–13** (0.150 g) in 3-chloropropionyl chloride (20 equiv) was refluxed for 2 h, cooled to 0 °C, filtered, and washed with ether. Recrystallization from ether gave the propanamides **14–23**.

2.1.3.1. N,N'-(2-(2-(Dimethylamino)ethyl)-1,3-dioxo-2,3-dihydro-1H-benzo[de]isoquinoline-5,8-diyl)bis(3-chloropropanamide) (14).

Yield: 93%. ¹H NMR (DMSO-*d*₆) 2.22 (s, 6H); 3.15 (t, 4H, *J* = 6.03 Hz); 3.52 (t, 2H, *J* = 7.45 Hz); 4.11 (t, 4H, *J* = 6.03 Hz); 4.52 (t, 2H, *J* = 7.45 Hz); 8.63 (d, 4H, *J* = 2.19 Hz); 10.81 (s, 2H).

2.1.3.2. N,N'-(1,3-Dioxo-2-(2-(pyrrolidin-1-yl)ethyl)-2,3-dihydro-1H-benzo[de]isoquinoline-5,8-diyl)bis(3-chloropropanamide) (15).

Yield: 96%. ¹H NMR (DMSO-*d*₆) 1.98 (br, 2H); 2.10 (br, 2H); 3.00 (t, 4H, *J* = 6.03 Hz); 3.11 (br, 2H); 3.53 (t, 2H, *J* = 7.45 Hz); 3.72 (br, 2H); 4.00 (t, 4H, *J* = 6.03 Hz); 4.49 (t, 2H, *J* = 7.45 Hz); 8.61 (s, 4H); 10.81 (s, 2H).

2.1.3.3. N,N'-(1,3-Dioxo-2-(2-(piperidin-1-yl)ethyl)-2,3-dihydro-1H-benzo[de]isoquinoline-5,8-diyl)bis(3-chloropropanamide) (16).

Yield: 96%. ¹H NMR (DMSO-*d*₆) 1.52 (br, 2H); 2.12 (br, 2H); 2.98 (br, 2H); 3.00 (t, 4H, *J* = 6.03 Hz); 3.20 (br, 2H); 3.52 (br, 2H); 3.88 (t, 4H, *J* = 6.03 Hz); 4.12 (br, 2H); 8.72 (s, 4H); 10.78 (s, 2H).

2.1.3.4. N,N'-(2-(2-Morpholinoethyl)-1,3-dioxo-2,3-dihydro-1H-benzo[de]isoquinoline-5,8-diyl)bis(3-chloropropanamide) (17).

Yield: 87%. ¹H NMR (DMSO-*d*₆) 2.95 (t, 4H, *J* = 6.03 Hz); 3.02 (m, 2H); 3.22 (m, 2H); 3.41 (m, 2H); 3.97 (t, 4H, *J* = 6.03 Hz); 4.01 (t, 4H, *J* = 5.45 Hz); 4.12 (t, 2H, *J* = 7.45 Hz); 8.62 (d, 4H, *J* = 2.19 Hz); 10.79 (s, 2H).

2.1.3.5. N,N'-(2-(2-(4-(3-Chloropropanoyl)piperazin-1-yl)ethyl)-1,3-dioxo-2,3-dihydro-1H-benzo[de]isoquinoline-5,8-diyl)bis(3-chloropropanamide) (18).

Yield: 97%. ¹H NMR (DMSO-*d*₆) 2.80 (t, 2H, *J* = 7.45 Hz); 3.00 (t, 4H, *J* = 6.03 Hz); 3.80 (t, 2H, *J* = 7.45 Hz); 3.78 (br, 2H); 3.88 (t, 4H, *J* = 6.03 Hz); 4.42 (br, 2H); 8.72 (s, 4H); 10.78 (s, 2H).

2.1.3.6. N,N'-(2-(3-(Dimethylamino)propyl)-1,3-dioxo-2,3-dihydro-1H-benzo[de]isoquinoline-5,8-diyl)bis(3-chloropropanamide) (19).

Yield: 80%. ¹H NMR (DMSO-*d*₆) 2.00 (m, 2H); 2.72 (s, 6H); 2.96 (t, 4H, *J* = 6.03 Hz); 3.13 (t, 2H, *J* = 7.45 Hz); 3.98 (t, 4H, *J* = 6.03 Hz); 4.12 (t, 2H, *J* = 7.45 Hz); 8.58 (d, 4H, *J* = 2.19 Hz); 10.78 (s, 2H).

2.1.3.7. N,N'-(1,3-Dioxo-2-(3-(pyrrolidin-1-yl)propyl)-2,3-dihydro-1H-benzo[de]isoquinoline-5,8-diyl)bis(3-chloropropanamide) (20).

Yield: 94%. ¹H NMR (DMSO-*d*₆) 1.82 (m, 2H) 1.98 (m, 2H); 2.10 (m, 2H); 3.00 (t, 4H, *J* = 6.03 Hz); 3.11 (br, 2H); 3.53 (t, 2H, *J* = 7.45 Hz); 3.62 (br, 2H); 3.94 (t, 4H, *J* = 6.03 Hz); 4.12 (t, 2H, *J* = 7.45 Hz); 8.61 (d, 4H, *J* = 2.19 Hz); 10.83 (s, 2H).

2.1.3.8. N,N'-(1,3-Dioxo-2-(3-(piperidin-1-yl)propyl)-2,3-dihydro-1H-benzo[de]isoquinoline-5,8-diyl)bis(3-chloropropanamide) (21).

Yield: 98%. ¹H NMR (DMSO-*d*₆) 1.52 (m, 2H); 1.95 (m, 2H), 2.12 (m, 2H); 2.94 (m, 2H); 3.02 (t, 4H, *J* = 6.03 Hz); 3.20 (m, 2H); 3.52 (t,

2H, *J* = 7.45 Hz); 3.88 (t, 4H, *J* = 6.03 Hz); 4.12 (t, 2H, *J* = 7.45 Hz); 8.72 (d, 4H, *J* = 2.19 Hz); 10.78 (s, 2H).

2.1.3.9. N,N'-(2-(3-Morpholinopropyl)-1,3-dioxo-2,3-dihydro-1H-benzo[de]isoquinoline-5,8-diyl)bis(3-chloropropanamide) (22).

Yield: 87%. ¹H NMR (DMSO-*d*₆) 2.02 (m, 2H); 2.92 (t, 4H, *J* = 6.03 Hz); 3.02 (m, 2H); 3.22 (m, 2H); 3.41 (m, 2H); 3.78 (t, 4H, *J* = 5.45 Hz); 3.97 (t, 4H, *J* = 6.03 Hz); 4.12 (t, 2H, *J* = 7.45 Hz); 8.62 (d, 4H, *J* = 2.19 Hz); 10.78 (s, 2H).

2.1.3.10. N,N'-(2-(3-(4-(3-Chloropropanoyl)piperazin-1-yl)propyl)-1,3-dioxo-2,3-dihydro-1H-benzo[de]isoquinoline-5,8-diyl)bis(3-chloropropanamide) (23).

Yield: 98%. ¹H NMR (DMSO-*d*₆) 2.10 (m, 2H); 2.80 (t, 2H, *J* = 7.45 Hz); 3.00 (t, 4H, *J* = 6.03 Hz); 3.80 (t, 2H, *J* = 7.45 Hz); 3.78 (br, 2H); 3.88 (t, 4H, *J* = 6.03 Hz); 4.42 (br, 2H); 8.72 (s, 4H); 10.78 (s, 2H).

2.1.4. General procedures for I–X

To a stirred suspension of **14–23** (0.150 g) in EtOH (5 mL), NaI (0.5 equiv) and pyrrolidine (8 equiv) were added. The mixture was stirred at reflux for 3 h and allowed to cool to room temperature.

2.1.4.1. N,N'-(2-(2-(Dimethylamino)ethyl)-1,3-dioxo-2,3-dihydro-1H-benzo[de]isoquinoline-5,8-diyl)bis(3-(pyrrolidin-1-yl)propanamide) (I).

The residue was chromatographed on silica gel using CHCl₃/MeOH/NH₄OH 9/1/0.5 as an eluent affording **I** in 60% yield. Mp 192.8 °C; ¹H NMR (CDCl₃) 2.00 (br, 8H); 2.40 (s, 6H); 2.67 (br, 6H); 2.81 (br, 8H); 2.97 (t, 4H, *J* = 6.03 Hz); 4.32 (t, 2H, *J* = 7.23 Hz); 6.86 (d, 2H, *J* = 8.99 Hz); 7.18 (d, 2H, *J* = 8.99 Hz); 8.12 (d, 2H, *J* = 2.19 Hz); 8.78 (d, 2H, *J* = 2.19 Hz); 11.80 (br, 2NH); ¹³C NMR (CDCl₃) 22.1, 24.5, 37.1, 43.8, 49.6, 51.9, 55.4, 119.9, 121.2, 131.8, 135.8, 162.1, 169.9; MS (ESI) *m/z*: 549.35; Anal. Calcd for C₃₀H₄₀N₆O₄: C, 65.67; H, 7.35; N, 15.32; O, 11.66. Found: C, 65.55; H, 7.41; N, 15.40; O, 11.50.

2.1.4.2. N,N'-(1,3-Dioxo-2-(2-(pyrrolidin-1-yl)ethyl)-2,3-dihydro-1H-benzo[de]isoquinoline-5,8-diyl)bis(3-(pyrrolidin-1-yl)propanamide) (II).

The residue was chromatographed on silica gel using CHCl₃/MeOH/NH₄OH 9/1/0.5 as an eluent affording **II** in 80% yield. Mp 192.8 °C; ¹H NMR (CDCl₃) 2.00 (br, 8H); 2.40 (s, 6H); 2.67 (br, 6H); 2.81 (br, 8H); 2.97 (t, 4H, *J* = 6.03 Hz); 4.32 (t, 2H, *J* = 7.23 Hz); 6.86 (d, 2H, *J* = 8.99 Hz); 7.18 (d, 2H, *J* = 8.99 Hz); 8.12 (d, 2H, *J* = 2.19 Hz); 8.78 (d, 2H, *J* = 2.19 Hz); 11.80 (br, 2NH); ¹³C NMR (CDCl₃) 24.1, 24.2, 30.5, 39.4, 51.7, 53.8, 54.1, 54.8, 122.2, 123.4, 134.3, 138.7, 164.4, 172.2; MS (ESI) *m/z*: 549.35; Anal. Calcd for C₃₂H₄₂N₆O₄: C, 66.88; H, 7.37; N, 14.62; O, 11.14. Found: C, 66.68; H, 7.44; N, 14.59; O, 11.09.

2.1.4.3. N,N'-(1,3-Dioxo-2-(2-(piperidin-1-yl)ethyl)-2,3-dihydro-1H-benzo[de]isoquinoline-5,8-diyl)bis(3-(pyrrolidin-1-yl)propanamide) (III).

The residue was chromatographed on silica gel using CHCl₃/MeOH/NH₄OH 9.5/0.5/0.25 as an eluent affording **III** in 70% yield. Mp 181.4 °C; ¹H NMR (CDCl₃) 1.45 (m, 2H); 1.6 (m, 4H); 2.00 (br, 8H); 2.48 (br, 4H); 2.52 (t, 2H, *J* = 7.23 Hz); 2.62 (t, 4H, *J* = 6.03 Hz); 2.77 (br, 8H); 2.87 (t, 4H, *J* = 6.03 Hz); 4.18 (t, 2H, *J* = 7.23 Hz); 8.12 (d, 2H, *J* = 2.19 Hz); 8.78 (d, 2H, *J* = 2.19 Hz); 11.78 (br, 2NH); ¹³C NMR (CDCl₃) 24.3, 24.5, 25.8, 35.6, 40.1, 51.5, 53.5, 55.9, 57.2, 122.3, 123.6, 134.3, 138.6, 164.6, 171.8; MS (ESI) *m/z*: 589.36; Anal. Calcd for C₃₃H₄₄N₆O₄: C, 67.32; H, 7.53; N, 14.27; O, 10.87. Found: C, 67.20; H, 7.66; N, 14.18; O, 10.91.

2.1.4.4. N,N'-(2-(2-Morpholinoethyl)-1,3-dioxo-2,3-dihydro-1H-benzo[de]isoquinoline-5,8-diyl)bis(3-(pyrrolidin-1-yl)propanamide) (IV).

The residue was chromatographed on silica gel using CHCl₃/MeOH/NH₄OH 9.5/0.5/0.25 as an eluent affording **IV** in 77% yield. Mp 186.0 °C; ¹H NMR (CDCl₃) 2.00 (br, 8H); 2.48 (br, 4H); 2.51 (t, 2H, *J* = 7.23 Hz); 2.70 (t, 4H, *J* = 5.92 Hz); 2.80 (br, 8H); 3.01 (t, 4H, *J* = 5.92 Hz); 3.66 (m, 4H); 4.25 (t, 2H, *J* = 7.23 Hz); 8.18 (d, 2H, *J* = 2.19 Hz); 8.79 (d, 2H, *J* = 2.19 Hz); 11.56 (br, 2NH); ¹³C NMR (CDCl₃) 23.4, 23.5, 32.7, 34.5, 38.5, 41.7, 45.4, 51.1, 52.0, 52.8, 53.1, 53.3, 54.5, 55.7, 121.8, 122.7, 133.6, 138.4, 164.0, 169.9, 171.5; MS (ESI) *m/z*: 592.66; Anal. Calcd for C₃₃H₄₄N₆O₅: C, 65.06; H, 7.17; N, 14.23; O, 13.54. Found: C, 65.19; H, 7.08; N, 14.39; O, 13.70.

2.1.4.5. N,N'-(1,3-Dioxo-2-(2-(4-(3-(pyrrolidin-1-yl)propanoyl)piperazin-1-yl)ethyl)-2,3-dihydro-1H-benzo[de]isoquinoline-5,8-diyl)bis(3-(pyrrolidin-1-yl)propanamide) (V).

The residue was chromatographed on silica gel using CHCl₃/MeOH/TEA 9.5/1/0.5 as an eluent affording **V** in 63% yield. Mp 124.0 °C; ¹H NMR (CDCl₃) 1.81 (br, 4H); 2.00 (br, 8H); 2.50–2.61 (m, 10H); 2.65 (t, 4H, *J* = 6.03 Hz); 2.70–2.88 (m, 12H); 2.95 (t, 4H, *J* = 6.03 Hz); 3.47 (br, 2H); 3.62 (br, 2H); 4.32 (t, 2H, *J* = 7.23 Hz); 8.17 (d, 2H, *J* = 2.19 Hz); 8.75 (d, 2H, *J* = 2.19 Hz); 11.95 (br, 2NH); ¹³C NMR (CDCl₃) 24.6, 24.8, 32.8, 35.1, 38.6, 42.3, 46.5, 52.3, 52.1, 54.2, 55.1, 55.7, 122.0, 122.3, 123.8, 124.2, 135.3, 138.1, 164.3, 170.2, 172.0; MS (ESI) *m/z*: 715.6; Anal. Calcd for C₄₀H₅₆N₈O₅: C, 65.91; H, 7.74; N, 15.37; O, 10.97. Found: C, 66.10; H, 7.58; N, 15.47; O, 10.70.

2.1.4.6. N,N'-(2-(3-(Dimethylamino)propyl)-1,3-dioxo-2,3-dihydro-1H-benzo[de]isoquinoline-5,8-diyl)bis(3-(pyrrolidin-1-yl)propanamide) (VI).

The residue was chromatographed on silica gel using CHCl₃/MeOH/NH₄OH 9.5/0.5/0.15 as an eluent affording **VI** in 80% yield. Mp 172.0 °C; ¹H NMR (CDCl₃) 1.98 (m, 2H); 2.02 (br, 8H); 2.43 (s, 6H); 2.61 (br, 6H); 2.82 (br, 8H); 2.97 (t, 4H, *J* = 6.03 Hz); 4.32 (t, 2H, *J* = 7.23 Hz); 6.86 (d, 2H, *J* = 8.99 Hz); 7.18 (d, 2H, *J* = 8.99 Hz); 8.12 (d, 2H, *J* = 2.19 Hz); 8.78 (d, 2H, *J* = 2.19 Hz); 11.78 (br, 2NH); ¹³C NMR (CDCl₃) 22.1, 24.5, 37.1, 43.8, 49.6, 51.9, 55.4, 119.9, 121.2, 131.8, 135.8, 162.1, 169.9; MS (ESI) *m/z*: 563.33; Anal. Calcd for C₃₁H₄₂N₆O₄: C, 66.17; H, 7.52; N, 14.94; O, 11.37. Found: C, 66.22; H, 7.69; N, 14.77; O, 11.21.

2.1.4.7. N,N'-(1,3-Dioxo-2-(3-(pyrrolidin-1-yl)propyl)-2,3-dihydro-1H-benzo[de]isoquinoline-5,8-diyl)bis(3-(pyrrolidin-1-yl)propanamide) (VII).

The residue was chromatographed on silica gel using CHCl₃/MeOH/NH₄OH 9.5/0.15/0.25 as an eluent affording **VII** in 88% yield. Mp 165.0 °C; ¹H NMR (CDCl₃) 1.82 (br, 4H); 2.00 (br, 10H); 2.61 (br, 4H); 2.67 (m, 6H); 2.81 (br, 8H); 2.97 (t, 4H, *J* = 6.03 Hz); 4.32 (t, 2H, *J* = 7.23 Hz); 8.13 (d, 2H, *J* = 2.19 Hz); 8.78 (d, 2H, *J* = 2.19 Hz); 11.78 (br, 2NH); ¹³C NMR (CDCl₃) 23.8, 24.2, 27.9, 35.1, 39.5, 52.2, 53.8, 54.5, 54.6, 122.0, 123.4, 134.2, 138.4, 164.5, 172.0. MS (ESI) *m/z*: 589.20; Anal. Calcd for C₃₃H₄₄N₆O₄: C, 67.32; H, 7.53; N, 14.27; O, 10.87. Found: C, 67.19; H, 7.44; N, 14.39; O, 10.91.

2.1.4.8. N,N'-(1,3-Dioxo-2-(3-(piperidin-1-yl)propyl)-2,3-dihydro-1H-benzo[de]isoquinoline-5,8-diyl)bis(3-(pyrrolidin-1-yl)propanamide) (VIII).

The residue was chromatographed on silica gel using CHCl₃/MeOH/NH₄OH 9.5/0.5/0.25 as an eluent affording **VIII** in 76% yield. Mp 178.0 °C; ¹H NMR (CDCl₃) 1.45 (m, 2H); 1.6 (m, 4H); 1.98 (m, 2H); 2.00 (br, 8H); 2.48 (br, 4H); 2.52 (t, 2H, *J* = 7.23 Hz); 2.62 (t, 4H, *J* = 6.03 Hz); 2.77 (br, 8H); 2.87 (t, 4H, *J* = 6.03 Hz); 4.18 (t, 2H, *J* = 7.23 Hz); 8.12 (d, 2H, *J* = 2.19 Hz); 8.78 (d, 2H, *J* = 2.19 Hz);

11.78 (br, 2NH); ¹³C NMR (CDCl₃) 24.5, 24.8, 25.7, 26.4, 35.2, 39.9, 51.8, 53.7, 55.1, 57.2, 122.0, 123.4, 134.2, 138.5, 164.2, 171.6; MS (ESI) *m/z*: 603.4; Anal. Calcd for C₃₄H₄₆N₆O₄: C, 67.75; H, 7.69; N, 13.94; O, 10.62. Found: C, 67.58; H, 7.77; N, 13.89; O, 10.50.

2.1.4.9. N,N'-(2-(3-Morpholinopropyl)-1,3-dioxo-2,3-dihydro-1H-benzo[de]isoquinoline-5,8-diyl)bis(3-(pyrrolidin-1-yl)propanamide) (IX).

Compound **IX** was obtained by recrystallization from EtOH (yield: 82%). Mp 192.0 °C; ¹H NMR (CDCl₃) 1.98 (m, 2H); 2.00 (br, 8H); 2.48 (br, 4H); 2.51 (t, 2H, *J* = 7.23 Hz); 2.70 (t, 4H, *J* = 5.92 Hz); 2.80 (br, 8H); 3.01 (t, 4H, *J* = 5.92 Hz); 3.66 (m, 4H); 4.25 (t, 2H, *J* = 7.23 Hz); 8.18 (d, 2H, *J* = 2.19 Hz); 8.78 (d, 2H, *J* = 2.19 Hz); 11.55 (br, 2NH); ¹³C NMR (CDCl₃) 23.3, 23.8, 24.9, 32.8, 34.7, 38.8, 41.5, 45.2, 51.3, 51.8, 52.7, 53.0, 53.2, 54.4, 55.9, 121.6, 122.8, 133.7, 138.2, 164.1, 169.8, 171.7; MS (ESI) *m/z*: 605.4; Anal. Calcd for C₃₃H₄₄N₆O₅: C, 65.54; H, 7.33; N, 13.90; O, 13.23. Found: C, 65.41; H, 7.18; N, 13.78; O, 13.41.

2.1.4.10. N,N'-(1,3-Dioxo-2-(3-(4-(3-(pyrrolidin-1-yl)propanoyl)piperazin-1-yl)propyl)-2,3-dihydro-1H-benzo[de]isoquinoline-5,8-diyl)bis(3-(pyrrolidin-1-yl)propanamide) (X).

The residue was chromatographed on silica gel using CHCl₃/MeOH/NH₄OH 9.5/1/0.5 as an eluent affording **X** in 63% yield. Mp 148.0 °C; ¹H NMR (CDCl₃) 1.81 (br, 4H); 1.98 (m, 2H); 2.00 (br, 8H); 2.38 (br, 4H); 2.50–2.6 (m, 8H); 2.63 (t, 4H, *J* = 6.03 Hz); 2.70–2.88 (m, 10H); 2.95 (t, 4H, *J* = 6.03 Hz); 3.47 (br, 2H); 3.62 (br, 2H); 4.32 (t, 2H, *J* = 7.23 Hz); 8.17 (d, 2H, *J* = 2.19 Hz); 8.75 (d, 2H, *J* = 2.19 Hz); 11.95 (br, 2NH); ¹³C NMR (CDCl₃) 24.2, 24.6, 25.2, 32.7, 34.8, 39.2, 51.6, 52.2, 53.1, 53.5, 53.8, 54.5, 56.1, 121.0, 121.8, 122.8, 123.2, 134.0, 138.8, 164.2, 170.3, 172.8; MS (ESI) *m/z*: 729.49; Anal. Calcd for C₃₉H₅₄N₈O₅: C, 65.52; H, 7.61; N, 15.67; O, 11.19. Found: C, 65.44; H, 7.51; N, 15.78; O, 11.08.

2.2. Preparation of DNA for the biophysical studies

Oligodeoxynucleotides used for biophysical experiments were synthesized on a Millipore Cyclone Plus DNA synthesizer using solid phase β-cyanoethyl phosphoramidite chemistry at 15 μmol scale and purified by standard methods. Quadruplex and duplex samples were prepared by dissolving the lyophilised oligonucleotide in a buffer solution containing 20 mM potassium phosphate, 70 mM KCl, 0.1 mM EDTA, at pH 7.0. The resulting solutions were heated at 90 °C for 5 min and subsequently allowed to slowly cool to room temperature. The solutions were then equilibrated for 24 h at 4 °C. The concentration of oligonucleotides was determined by UV adsorption measurements at 90 °C using molar extinction coefficient values ε_(260nm) of 228,500 and 110,700 M⁻¹ cm⁻¹ for AGGG(TTAGGG)₃ and CGCGAATTCGCG, respectively. The molar extinction coefficient was calculated by the nearest neighbour model.²⁹

2.3. Fluorescence titrations

Fluorescence titrations were performed on a Perkin Elmer LS50B fluorescence spectrometer, using a 1 cm path length quartz cuvette. The ligands were dissolved in DMSO to produce stock solutions at 0.001 M (concentration was calculated using their respective molecular weights) and then diluted into the appropriate amount of aqueous buffer to yield a ligand concentration of 10 μM and a final DMSO concentration of 2%. In each titration, volumes of 5 or 10 μL of quadruplex solution at a concentration of 100–160 μM were added into a ligand solution (500 μL). After each addition of DNA, the solution was stirred and allowed to equilibrate for at least 3 min and fluorescence emission spectra were col-

lected from 400 to 600 nm, at 10 nm excitation and emission slit widths. Each experiment was performed at least three times, each spectrum was recorded three times and the average of three scans was taken. The fraction of free ligand (α) was calculated for each sample, following the changes in fluorescence emission maximum upon quadruplex addition, using the following relationship:

$$\alpha = \frac{F_{\max} - F_{\max}^b}{F_{\max}^f - F_{\max}^b}$$

where F_{\max} is the maximum fluorescence intensity observed, F_{\max}^f and F_{\max}^b are the respective fluorescence intensities of free ligand and fully bound ligand, respectively. To obtain the binding constants, the resulting titration curves, obtained by plotting the fraction of free ligand versus quadruplex concentration, were fitted with the ORIGIN 7.0 program by using the following equation.³⁰

$$\alpha = \left(\frac{1}{2L_0} \right) \left[\left(L_0 + nQ + \frac{1}{K_b} \right) - \sqrt{\left(L_0 + nQ + \frac{1}{K_b} \right)^2 - 4L_0nQ} \right]$$

where L_0 is the total ligand concentration, Q the added G-quadruplex concentration, n the number of binding sites and K_b the binding constant.

2.4. Isothermal titration calorimetry

ITC experiments were performed at 298 K using a high-sensitivity CSC-5300 Nano-ITC microcalorimeter from Calorimetry Science Inc. (Lindon, Utah) with a cell volume of 1 ml. Ligand solutions were prepared by dissolving the powder in the same buffer used for DNA, and the concentration has been estimated by UV spectroscopy using the calculated extinction coefficients (Table S1). Measurement from the first injection was discarded from the analysis of the data, to avoid artifacts due to the diffusion through the injection port occurring during the equilibration period, locally affecting the quadruplex concentration near the syringe needle tip. In each titration, volumes of 5–10 μ L of ligand solution at a concentration of 480–640 μ M were injected into a quadruplex or duplex solution (30–40 μ M) every 300 or 400 s up to a total of 25–50 injections, using a computer-controlled 250 μ L microsyringe, with stirring at 150 rpm. Heat produced by ligands dilution was evaluated by performing ligand dilution experiment, titrating each ligand into the buffer alone. The interaction heats were calculated after correction for the heat of ligand dilution. The corrected heat values were plotted as a function of the molar ratio, to give the corresponding binding isotherms. The resulting isotherms were fitted with an independent and equivalent-sites model or a multiple-sites model employing a nonlinear least-squares minimization algorithm, by using the Bindwork software from Calorimetry Science Inc., to give the binding enthalpy ($\Delta_b H^\circ$), binding constant (K_b) and stoichiometry (n). The Gibbs energy change and the entropic contribution were calculated using the relationships $\Delta_b G^\circ = -RT \ln K_b$ ($R = 8.314 \text{ J mol}^{-1} \text{ K}^{-1}$, $T = 298 \text{ K}$) and $T\Delta_b S^\circ = \Delta_b H^\circ - \Delta_b G^\circ$. Each ITC experiment was performed at least three times.

2.5. Circular dichroism

CD spectra were recorded with a Jasco J-715 spectropolarimeter equipped with a Peltier-type temperature control system (model PTC-348WI) and calibrated with an aqueous solution of 0.06% d-10-(1)-camphorsulfonic acid at 290 nm. CD spectra of quadruplex DNA solutions (40 μ M) and of solutions containing DNA in the presence of an excess of ligand were recorded between 220 and 340 nm, using 1 mm path-length cuvettes and were averaged over three scans. Buffer baseline was subtracted from each spectrum. A

time constant of 4 s, a 2 nm bandwidth, and a scan rate of 20 nm min^{-1} were used to acquire the data.

2.6. UV-melting experiments

UV-melting experiments were carried out using a Jasco V-530 UV-visible spectrophotometer equipped with a Jasco ETC-505-T temperature controller. Solutions of quadruplex DNA (25 μ M) and of 1:1 or 2:1 ligand/DNA mixture samples (300 μ L) were placed in quartz cuvettes of 1 mm path length. UV-melting experiments were performed in a temperature range of 20–85 $^\circ\text{C}$ by monitoring absorbance at 295 nm,³¹ at a 0.5 $^\circ\text{C}/\text{min}$ heating rate. Each experiment was performed at least three times. Thermal denaturation temperatures (T_m) for the DNA and DNA–ligand complexes were determined using previously reported procedure,³² and represent the mean \pm SD.

2.7. Enzyme assays. Telomeric repeat amplification protocol (TRAP assay) on A549 cells

Telomerase activity was evaluated by Telomeric Repeat Amplification Protocol (TRAP) assay using the TeloTAGG Telomerase PCR ELISAPLUS (Roche Diagnostics)³³ which is an extension of the original method described by Kim et al.³⁴ Cell extract ($1\text{--}3 \times 10^5$ cell equivalents), at 72 h post exposure to examined compounds, in different concentrations, were employed in the first step, in which telomerase adds telomeric repeats (TTAGGG) to the 3'-end of the biotin-labeled synthetic P1-TS primer, according to manufacturer's protocol for the TeloTAGG Telomerase PCR ELISA^{PLUS} kit analysis. Briefly, reaction mixtures contained telomerase extracts, oligonucleotide primers (P1-TS and P2) for amplification of telomeric repeats and internal standard (IS), Taq DNA polymerase (5 units/ μ L) (Roche), dNTP Mix and TRAP reaction buffer. After 20 min incubation at 25 $^\circ\text{C}$ for telomerase extension of the P1-TS primer, the PCR cycling conditions were 94 $^\circ\text{C}$ for 5 min followed by 30 cycles at 94 $^\circ\text{C}$ for 30 s, 50 $^\circ\text{C}$ for 30 s and 72 $^\circ\text{C}$ for 90 s with final step at 72 $^\circ\text{C}$ for 10 min. The PCR products derived from telomerase elongation and internal standard are quantitatively determined using ELISA assay. The ELISA kit allows the highly specific amplification of telomerase-mediated elongation products combined with non-radioactive detection following an ELISA protocol. The levels of telomerase activity were within the linear range of the TRAP assay. A heat-inactivated cell extract was also tested as a negative control. Data are presented as mean \pm SEM. The paired Student's *t*-test was used for comparison between control and experimental groups. *P* value <0.05 was considered statistically significant.

2.8. Biological evaluation-cell growth inhibition and toxicity assays

M14 human melanoma and A549 human lung cancer cell lines were maintained in logarithmic growth phase at 37 $^\circ\text{C}$ in a 5% CO_2 humidified atmosphere in RPMI-1640 medium containing 10% fetal calf serum, 2 mM of L-glutamine and 0.1 mg/ml gentamycin. Compounds, synthesized as previously described, were reconstituted in sterile DMSO and then diluted with sterile water to the desired concentrations, immediately before each experiment. To evaluate the toxic profiles of the potential antitelomeric compounds, a colorimetric assay was used as described by Mosmann.³⁵ The assay is based on the tetrazolium salt 3-(4,5-dimethylthiazolyl-2)-2,5-diphenyltetrazoliumbromide (MTT), (Sigma, Milan, Italy) a pale yellow substrate that is cleaved by active mitochondria to produce a dark blue formazan product. MTT assays were performed as follows: cells were plated in 96-well plates at 1000–3000 cells/well and allowed to attach for 24 h. Cells were exposed to 0.1–100 μ M of drugs at 37 $^\circ\text{C}$ for 5 days. In each experiment con-

trol samples were run with 0.2% DMSO. At the end of this period, MTT was added to a final concentration of 50 $\mu\text{g}/\mu\text{L}$, and four additional hours of incubation were performed. After that, medium was aspirated carefully and 100 μL of acidified isopropanol was added per well. Soluble formazan salts were homogenized by manual pipetting and absorbance at 570 nm was read. Each experimental point was run eight times. The results were expressed as the absorbance values of treated samples compared with those of controls. The *in vitro* activity of the drugs was expressed in terms of concentration able to inhibit cell proliferation by 50% (IC_{50}). IC_{50} values were determined graphically from the growth inhibition curves obtained after 5 days of exposure of the cells to each drug. Data represent mean values \pm SD of three independent experiments. The same procedure applied in the case of A549 and M14 cell lines was conducted for normal fibroblasts NIH3T3 (mouse embryo fibroblast), except for using bovine calf serum (BCS) instead of FBS.

3. Results and discussion

3.1. Chemistry

Synthesis of the trifunctionalized derivatives **I–X** (Scheme 1) was accomplished using procedures described in Scheme 2. The key intermediate, 3,6-diamino-1,8-naphthalic anhydride (**3**), was obtained from 3-nitro-1,8-naphthalic anhydride (**1**), which was subjected to nitration followed by reduction of both nitro groups to obtain intermediate **3**. Intermediate **3** was treated with the opportune amines to provide naphthalimides **4–13**. Amines 3-(piperidin-1-yl)propan-1-amine and *tert*-butyl 4-(3-aminopropyl)piperazine-1-carboxylate, were prepared according to the procedure described in the literature.^{36,37} The remaining amines were commercially available. Acylation of diamines **4–13** by 3-chloropropionyl chloride and subsequent aminolysis by reflux treatment with pyrrolidine, in the presence of NaI as catalyst, gave the desired derivatives **I–X**. Compounds were obtained in good yields and were adjudged pure by elemental analysis, mass spectrometry, ^1H and ^{13}C NMR.

It should be underlined that all tested compounds have side chains bearing pyrrolidine rings ($\text{pK}_a \approx 11$), that can be considered totally charged in the experimental conditions we adopted in titration experiments (pH 7.0) (see below). Similar considerations can be made for side chains containing piperidine rings (**III** and **VIII**) and dimethylamino moieties (**I** and **VI**) for which a comparable pK_a could be envisaged. On the other hand, for compounds characterized by side chains containing a morpholine ring (**IV** and **IX**), the expected pK_a (about 8) provide about 90% of charged chains.

3.2. Biophysical analysis

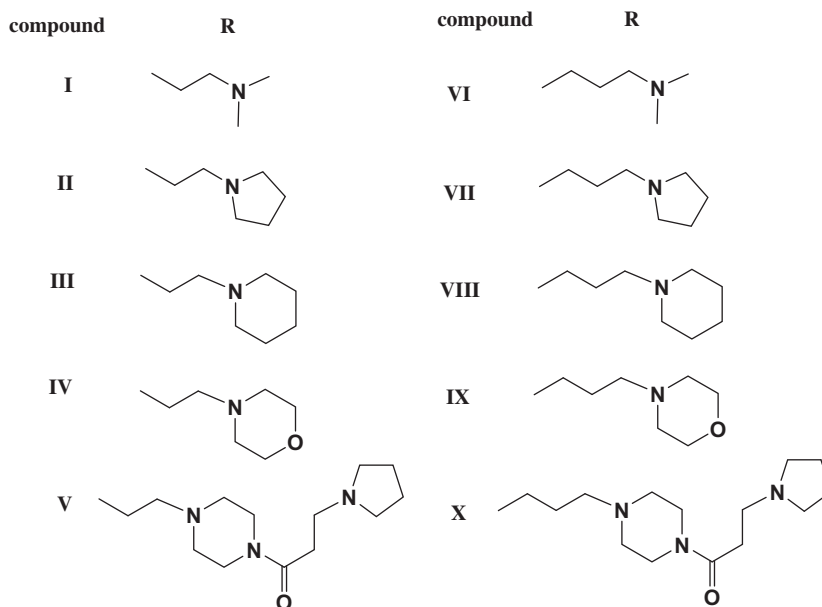
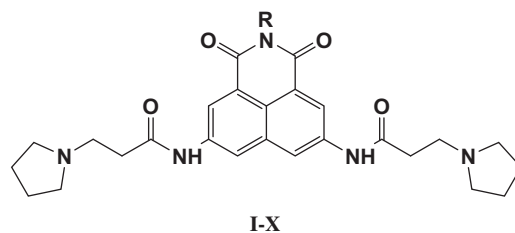
Fluorescence emission spectra of naphthalimido derivatives in the absence and presence of increasing amounts of quadruplex were recorded in order to screen such collection of molecules for their quadruplex affinity. Fluorescence titration experiments were performed with the quadruplex-forming human telomeric sequence AGGG(TTAGGG)₃, already used in similar investigations,^{30,38} under experimental conditions highly favorable to quadruplex formation (70 mM KCl),³⁹ arguing against binding to the single-stranded form of oligonucleotide. Naphthalimido derivatives show fluorescence quenching when binding to quadruplex DNA. The binding constants were determined from the variation of fluorescence properties. The binding curves for all the systems were obtained by plotting the fraction of free ligand versus quadruplex concentration (Fig. 1). The resulting titration curves were fitted using the independent and equivalent-sites model (see Section 2). Fluorescence titrations showed that eight out of ten com-

pounds have capability for binding to quadruplex DNA and that compounds **VII** and **VIII** show the best affinity for the quadruplex (Table 1). Our experimental results suggest that the length of the chain seems to be important for quadruplex-binding ability of these drugs, indicating the derivatives with propyl chains as the ones with more affinity for the quadruplex. Fluorescence titration data showed that the binding to the quadruplex structure AGGG(TTAGGG)₃ varied over a fivefold range between the strongest compound **VII** ($K_b = 30 \times 10^5 \text{ M}^{-1}$) and weakest compound **I** ($K_b = 6 \times 10^5 \text{ M}^{-1}$). The results of the interpolation analysis indicate that the data concerning the compounds **VII** and **VIII** could not be fitted with a single binding site, but they are well fitted with two independent binding sites per quadruplex molecule.

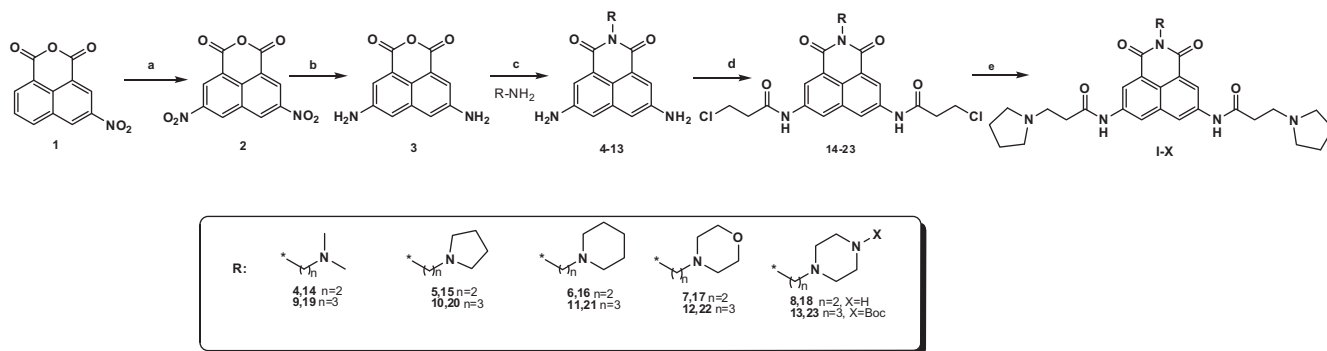
In order to obtain a complete thermodynamic characterization of the interaction between the best naphthalimido derivatives (compounds **VII** and **VIII**) and human telomeric quadruplex, and to evaluate the individual binding constants, a calorimetric analysis has been carried out by means of isothermal titration experiments. Indeed, ITC is a high-accuracy method for the measurement of thermodynamic parameters in biological interactions and it is the only technique capable of quantifying both enthalpic and entropic components of the interaction, revealing the overall nature of the forces that drive the molecular recognition.⁴⁰ ITC has been used to characterize the energetics of several drug–quadruplex interactions,^{41–44} and it has been successfully applied to extract the individual binding constants when the binding process comprises two sequential events resulting in the formation of a complex.^{45,46}

To gain a deeper understanding of the quadruplex-binding behaviour of these analogues, a direct comparison with the binding behaviour of compound **IX** was performed. Compound **IX** was selected for the successive ITC study because it belongs to the series with propyl side-chain moieties, as compounds **VII** and **VIII** that showed the highest binding constants. Examples of the raw ITC and integrated heat data for the titration of human telomeric quadruplex with compounds **VII**, **VIII** and **IX** are shown in Figure 2. The raw ITC data (insets in Fig. 2) indicate exothermic interactions. In all cases, with each injection of ligand, less and less heat release was observed until constant values were obtained, reflecting a saturable process. The normalized heat binding curves of compounds **VII** and **VIII** (Fig. 2, panels A and B) show biphasic profiles, with two separate binding events, well fitted using a multiple-sites model. In the first event, one molecule of ligand interacts with the quadruplex structure, followed by the binding of a further ligand molecule, allowing the formation of a final complex composed of one molecule of quadruplex and two molecules of ligand. The analysis suggests that the first binding event ($K_b = 2 \times 10^7 \text{ M}^{-1}$ and $5 \times 10^7 \text{ M}^{-1}$ for **VII** and **VIII**, respectively) is about two order of magnitude stronger than the second one ($K_b = 5 \times 10^5 \text{ M}^{-1}$ and $6 \times 10^5 \text{ M}^{-1}$ for **VII** and **VIII**, respectively). Considerably different results were obtained for the interaction of compound **IX**. Indeed, the binding isotherm of compound **IX** (Fig. 2, panel C) shows a simpler profile compared to the ones of **VII** and **VIII**, with a single sigmoidal curve centered at 1:1 stoichiometry. The binding curve obtained is, in this case, well fitted using an independent and equivalent-sites model. The analysis of the binding isotherm of **IX** suggests that the affinity of this compound for the quadruplex ($K_b = 4 \times 10^5 \text{ M}^{-1}$) is comparable with the one measured for the second binding event of **VII** and **VIII**.

The values of K_b and $\Delta_b H^\circ$ derived by ITC enable us to complete the thermodynamic characterization by calculating corresponding values of $T\Delta_b S^\circ$ and $\Delta_b G^\circ$. The resulting thermodynamic parameters are showed in Table 2. In the case of **VII** and **VIII**, the thermodynamic profiles of the ligand–quadruplex interactions are qualitatively similar. Inspection of the data reveals that the two binding events of **VII** and **VIII** are driven by both enthalpic and



Scheme 1. Chemical structures of compounds I-X.



Scheme 2. Reagents and conditions: (a) $\text{H}_2\text{SO}_4/\text{HNO}_3$, from -10°C to 55°C , 1 h; (b) HCOONH_4 , Pd(C), DMF/MeOH, rt, 2 h; (c) toluene/EtOH, Δ , 2 h; (d) 3-chloropropionyl chloride, Δ , 2 h; (e) pyrrolidine, NaI, EtOH, Δ , 2.5 h.

entropic contributions, as well as the single binding event of compound **IX**. However, the enthalpic component for the binding of **IX** is more favourable than the other two ligands, probably because the oxygen atom of the morpholinopropyl side-chain is able to gain an additional H-bond with DNA. This could lead to the formation of a more rigid complex with respect to the others, consistent with the low entropic contribution observed by ITC.

The ITC data confirm that **VII** and **VIII** interact with quadruplex DNA more avidly than **IX**. Inspection of Tables 1 and 2 shows that the K_b values determined from the fluorescence and ITC data differ, despite the use of identical salt and buffer conditions. To explain those apparent discrepancies, some considerations need to be done. A binding constant can be accurately determined when the

titrant, for example, a ligand, is added to a fixed and constant concentration of DNA (or vice versa), such that this concentration is in the range of $1/K_b$. In fluorescence titrations, the concentration used ($10\ \mu\text{M}$) is closer to $1/K_b$ (about $1\ \mu\text{M}$) than the one used in ITC ($30\text{--}40\ \mu\text{M}$). Thus, in the case of **IX** (1:1 stoichiometry), we should consider the spectroscopic binding constant more accurate than the calorimetric one. On the other hand, in the case of **VII** and **VIII** (2:1 stoichiometry), thanks to ITC we were able to extract the individual binding constants associated to each binding event, whereas, by fluorescence we observe almost certainly an average of the two constants.

To investigate the selectivity of compounds **VII** and **VIII**, the binding of these compounds to duplex DNA was preliminary eval-

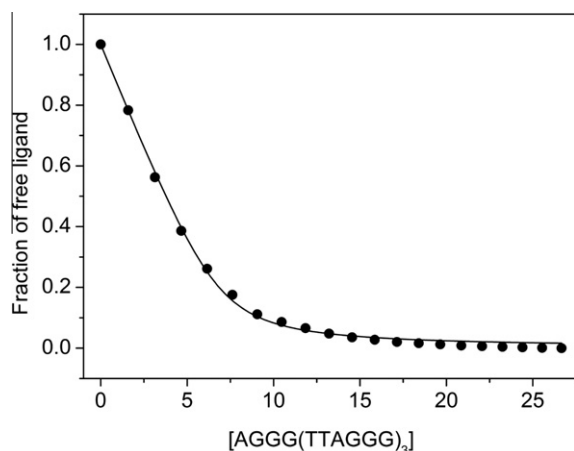


Figure 1. Example of fluorescence titration curve for compound **VII** (10 μM), obtained by plotting the fraction of free ligand as a function of quadruplex concentration (μM). The experimental data (circles) are fitted using an independent and equivalent-sites model (solid line) to obtain the binding constants. All the titration experiments were performed at 25 °C in buffer solution containing 20 mM potassium phosphate, 70 mM KCl, 0.1 mM EDTA, at pH 7.0.

Table 1

Binding constants for the interaction of naphthalimido derivatives with quadruplex AGGG(TTAGGG)₃ determined by fluorescence titrations

Compound	$K_b \times 10^5 \text{ (M}^{-1}\text{)}$	Compound	$K_b \times 10^5 \text{ (M}^{-1}\text{)}$
I	6 ± 1	VI	nd
II	12 ± 2	VII	30 ± 3
III	9 ± 1	VIII	24 ± 3
IV	nd	IX	10 ± 1
V	7 ± 1	X	9 ± 1

nd = not detected.

uated by UV titration experiments with the genomic STDNA, which was selected as it presents 42% of GC bases and it is commonly regarded as a reference duplex. UV studies have indicated a low affinity of **VII** and **VIII** for duplex structure (data not shown), suggesting that the two compounds have preference for the quadruplex structure over the duplex.

Additionally, in order to support these results, we evaluated the affinity of **VII** for the duplex model formed by the Dickerson sequence CGCGAATTCGCG by ITC (Fig. S1). The binding constant obtained ($5 \times 10^5 \text{ M}^{-1}$, Table S2) is about two orders of magnitude lower than for AGGG(TTAGGG)₃ quadruplex, thus confirming the preference for the quadruplex structure.

Furthermore, CD experiments were carried out to evaluate if the structure of the quadruplex is maintained upon ligands addition. The investigated quadruplex-forming sequence shows the typical CD spectrum of the hybrid conformation (Fig. 3), with a maximum around 290 nm, a shoulder centered around 270 nm and a weak minimum around 240 nm.⁹ The addition of **VII**, **VIII** or **IX** causes the increase of the shoulder at 270 nm in the CD spectra, thus suggesting that the structure of the quadruplex is maintained upon ligands addition, although their interaction could promote some conformational changes in the quadruplex DNA structure.

In order to test the ability of the ligands to stabilize quadruplex upon binding, thermal denaturation experiments were performed, as well. Since quadruplex structure melts with a characteristic hypochromic shift at 295 nm,³¹ UV-melting experiments were performed by recording the absorbance at that wavelength. The experiments were carried out at two different ligand/DNA ratio (1:1 and 2:1). All the UV-melting profiles were consistent with

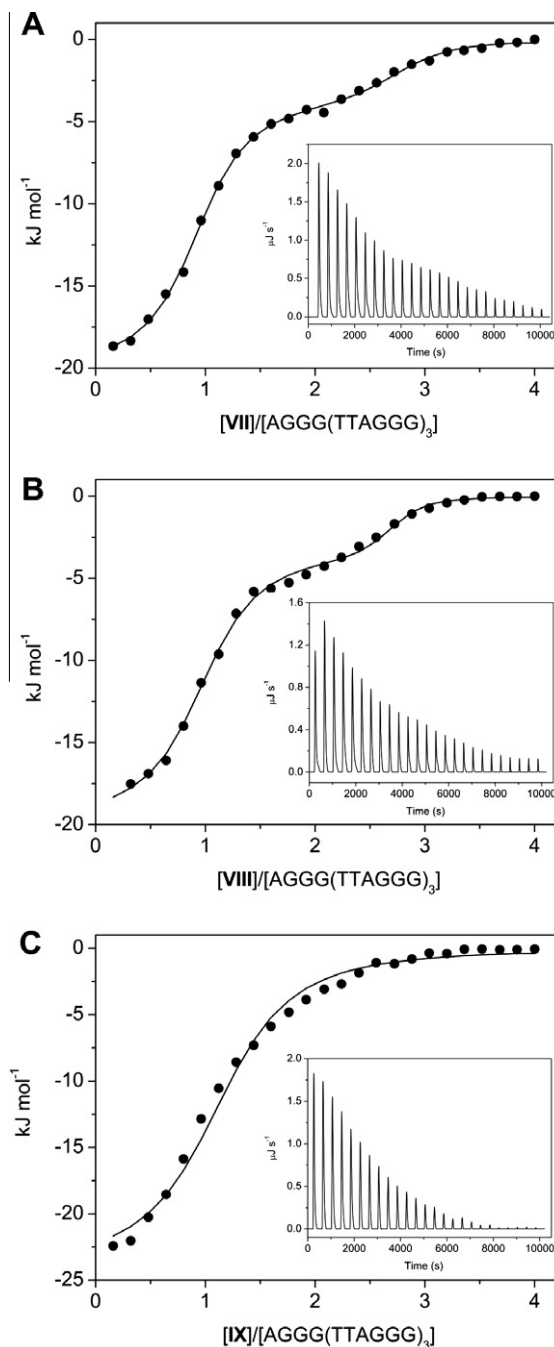
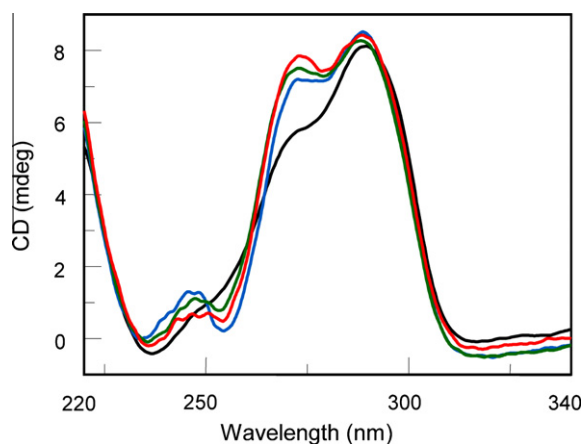


Figure 2. Raw ITC data (insets) and binding isotherms for titration of AGGG(TTAGGG)₃ quadruplex with compounds **VII** (A), **VIII** (B) and **IX** (C), obtained at 25 °C in a buffer solution containing 20 mM potassium phosphate, 70 mM KCl, 0.1 mM EDTA, at pH 7.0. The circles represent the experimental data obtained by integrating the raw ITC data and subtracting the heat of ligand dilution into the buffer. The line represents the best fit obtained by a nonlinear least-squares procedure based on a multiple-sites model (A and B) and on an independent and equivalent-sites model (C).

the G-quadruplex folding (Fig. S2). Relative stabilities of the quadruplexes upon ligand binding are reported in Table 3. In all the cases, the addition of one equivalent of ligand to quadruplex DNA solutions leads to T_m values higher than the uncomplexed quadruplex ($\Delta T_m = 3 \text{ }^\circ\text{C}$). In the cases of **VII** and **VIII**, the addition of two equivalents of ligand leads to a further enhancement of T_m values (62 and 63 °C, respectively). On the other hand, in the case of **IX** the T_m value at 2:1 ligand/DNA ratio is indistinguishable

Table 2Thermodynamic parameters for the interaction of naphthalimido derivatives with AGGG(TTAGGG)₃ quadruplex determined by ITC at 25 °C and pH 7.0^a

Compd	First binding event					Second binding event				
	n_1^b	K_b (M ⁻¹)	$\Delta_b H^\circ$ (kJ mol ⁻¹)	$-T\Delta_b S^\circ$ (kJ mol ⁻¹)	$\Delta_b G_{298K}^\circ$ (kJ mol ⁻¹)	n_2^b	K_b (M ⁻¹)	$\Delta_b H^\circ$ (kJ mol ⁻¹)	$-T\Delta_b S^\circ$ (kJ mol ⁻¹)	$\Delta_b G_{298K}^\circ$ (kJ mol ⁻¹)
VII	1	2×10^7	-19	-23	-42	1	5×10^5	-6	-26	-32
VIII	1	5×10^7	-18	-26	-44	1	6×10^5	-6	-27	-33
IX	1	4×10^5	-23	-9	-32					

^a The experimental error for each thermodynamic parameter is <8%.^b n_1 and n_2 are referred to the number of ligand molecules interacting in each binding event; the final stoichiometry of the complexes is $n_{tot} = n_1 + n_2$.**Figure 3.** CD spectra of AGGG(TTAGGG)₃ quadruplex-forming sequence before (black line) and after the addition of an excess of **VII** (red line), **VIII** (blue line) and **IX** (green line). All the spectra were recorded at 25 °C in a buffer solution containing 20 mM potassium phosphate, 70 mM KCl, 0.1 mM EDTA, at pH 7.0.

from the one at 1:1 ratio ($T_m = 60$ °C). Our thermal denaturation results confirm that two molecules of **VII** and **VIII** bind and stabilize the human telomeric quadruplex structure, whereas, in the case of **IX**, just one molecule interacts with the investigated quadruplex.

In summary, fluorescence titration experiments allowed us to screen a collection of naphthalimido derivatives for binding affinity to the quadruplex structure formed by the human telomeric sequence. The combination of spectroscopic and calorimetric results enabled us to shed light on the recognition processes between the quadruplex and the derivatives showing the higher affinity. ITC experiments showed that, from a thermodynamic point of view, the interactions of the best naphthalimido derivatives with the quadruplex are strongly favoured and that the final stoichiometry of the complexes is 2:1 (ligand/DNA). Interestingly, ITC experiments reveal that the two molecules of ligand do not simultaneously bind the quadruplex structure, but the interaction is sequential and composed by two distinct binding events. CD and UV experiments revealed that the structure of the quadruplex is preserved upon binding and that the drugs are also able to induce quadruplex stabilization.

Table 3Melting temperatures for AGGG(TTAGGG)₃ quadruplex-forming sequence (TQ) and 1:1 or 1:2 DNA/ligand mixture samples calculated from UV-melting curves recorded at 295 nm

Sample	T_m (°C) (± 0.2)
TQ	57.0
TQ + VII (1:1)	60.0
TQ + VII (1:2)	63.0
TQ + VIII (1:1)	60.0
TQ + VIII (1:2)	62.0
TQ + IX (1:1)	60.0
TQ + IX (1:2)	60.0

3.3. Evaluation of TRAP-inhibitory activity

Compounds **VII**, **VIII** and **IX**, were also tested as telomerase inhibitors.^{47–49} As shown in Figure 4, after 72 h of exposure, we obtained a significant decrease of telomerase activity (black bars) for all the compounds tested in a dose-dependent manner, with an appreciable selectivity comparing to Taq polymerase inhibition (white bars) calculated from internal standard level amplification quantification for compounds **VII** and **VIII**. In particular, in the presence of 5 μ M of compound **VII**, we detected reducing values of 50%. In the presence of 5 μ M of **VIII** telomerase activity has been reduced of 26%. According to the results shown in Figure 4 we observed that in the range of concentrations 0.1–50 μ M, compound **VII** decreased the activity of telomerase with an appreciable selectivity comparing to Taq polymerase inhibition. At higher concentrations of compound **VIII** (10–100 μ M) the inhibition of Taq polymerase is also observed with a loss in selectivity. For compound **IX** no selectivity between telomerase and Taq polymerase inhibition has been detected. These results are consistent with the studies about the interaction drug/quadruplex in which compounds **VII** and **VIII** showed the best binding constants towards telomeric quadruplex.

3.4. Cell cytotoxicity

Antiproliferative experiments were carried out in order to get some insights on the in vitro properties of the best binding compounds, namely **VII** and **VIII**, and compound **IX**, as well, against the lung cancer A549 and the human melanoma M14 cell lines, when these were exposed to different drug concentrations (from 0.1 to 100 μ M) for 5 days. We have selected these two cell lines because they are the most widely studied cells among non-small cell lung carcinoma and melanoma panels, respectively. Moreover, M14 Melanoma cells are still a valuable model for investigating cancer metastasis.⁵⁰ A marked dose-dependent inhibition of cell growth was consistently observed in both cell lines. The detailed profile of the inhibition of these cell lines by our compounds is reported in Figure 5.

The aim of this experiment was to evaluate cell growth as a function of drug concentration and to calculate the IC₅₀ values as detailed in the experimental section. The obtained results are summarized in Table 4, with IC₅₀ values ranging from 1.5 to 34.7 μ M in M14 melanoma cells and from 5.15 to 40.3 μ M in A549 lung cancer cells. Generally, the in vitro experiments revealed a good activity of tested compounds. In particular, M14 melanoma cells appeared to be more sensitive to the growth inhibition by tested compounds than A549 lung cancer cells. The most interesting result was related to compound **VII**, which was found to be the best inhibitor of this series against both M14 and A549 cell lines with IC₅₀ of 1.5 ± 0.7 and 5.15 ± 0.91 , respectively. Moreover, selected compounds were tested against NIH3T3 normal fibroblasts in order to determine their selectivity for cancer cells compared with normal cells. Compounds **VII** and **VIII** showed higher selectivity for A549 and M14 cells than for NIH3T3 fibroblasts. On the other hand, compound **IX**, showing a better affinity towards DNA duplex, is

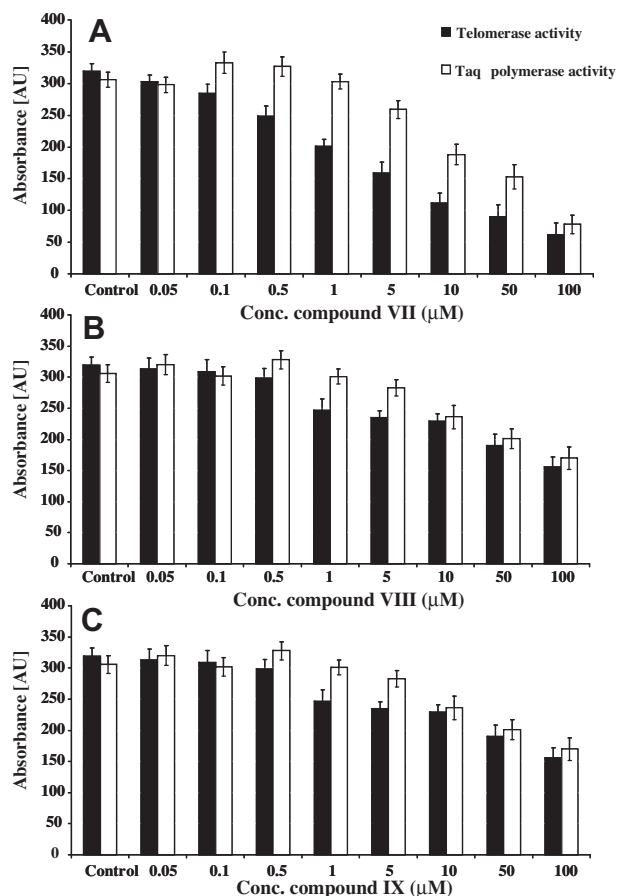


Figure 4. Effect of the increasing concentrations of compounds **VII** (A), **VIII** (B) and **IX** (C) on the human telomerase activity, represented by the absorbance measurements following the ELISA protocol in TRAP assay. TRAP assay was performed on the extract of A549 cells exposed for 72 h to the examined compounds. All experiments were performed in triplicates, and error bars show the standard error of the mean values (\pm SEM). Black bars, telomerase activity; white bars, Taq polymerase activity.

toxic for NIH3T3 fibroblasts. So it can be concluded that derivatives **VII** and **VIII** are promising leads for design of highly potent and highly selective anti-proliferative agent for treatment of melanoma and lung cancer.

4. Conclusions

G-Quadruplex ligands based on the trisubstituted naphthalimido aromatic nucleus have been synthesized and evaluated as telo-

Table 4

In vitro results of selected compounds against melanoma (M14), lung (A549) cancer cell lines and normal fibroblasts (NIH3T3) expressed as IC_{50} in μ M.

Cpd	M14 (μ M + S.D.)	A549 (μ M + S.D.)	NIH3T3 (μ M + S.D.)
VII	1.5 \pm 0.7	5.2 \pm 0.9	NOT ACTIVE
VIII	8.0 \pm 0.8	9.9 \pm 1.8	43.3 \pm 4.3
IX	34.7 \pm 0.6	40.3 \pm 1.6	4.6 \pm 0.1

meric binding agents. An initial screening, performed by fluorescence titration experiments involving the telomeric quadruplex AGGG(TTAGGG)₃, has allowed us to select two compounds showing the best affinities (**VII** and **VIII**), to be further investigated. Isothermal titration calorimetry measurements strongly suggest that **VII** and **VIII** are able to bind the telomeric quadruplex with a drug/DNA ratio 2:1. In both cases the association constants for the 1:1 complexes are two orders of magnitude higher than those for the 2:1 complexes. On the other hand, data for derivative **IX** point only to the formation of a 1:1 drug/DNA complex characterized by an association constant two order of magnitude lower compared to **VII** and **VIII**. Interestingly, the interaction stoichiometry of compounds **VII** and **VIII** with the telomeric quadruplex AGGG(TTAGGG)₃ is similar to that observed for drug BRACO-19⁵¹ that was shown to inhibit tumour growth consistently with telomere targeting.⁵² Derivatives **VII** and **VIII** have been further evaluated for their ability to inhibit telomerase by a TRAP assay. Particularly, compound **VII** comes out more active and selective than the other ones. Described results have encouraged us to estimate their cell toxicity against the lung cancer A549 and the human melanoma M14 cell lines. Compound **VII** shows the best activity for both cell lines and is not toxic for normal cell line. These results are in good agreement with data collected both from physico-chemical measurements and TRAP assays. Recently, the properties of a series of tetrasubstituted naphthalene diimide derivatives has been reported,⁵³ that have been shown to be more active than compound **VII** against the lung cancer A549 cell lines. However it should be noted that these compounds are characterized by four substituents and side chains different from those ones introduced in our compounds. It is our intention take into consideration these results in designing new derivatives. In conclusion, our results show that trisubstituted naphthalimido derivatives are a promising class of ligands able to bind telomeric G-quadruplex and to remarkably inhibit telomerase, thus supporting the potential of this class of quadruplex-interactive compounds for use in anticancer approaches. On the basis of these findings molecular modelling will be envisaged towards the development of drugs characterized by higher affinities to telomeric G-quadruplex structures and endowed by higher antiproliferative properties. As a matter of fact, the described synthetic approach for their preparation is quite ver-

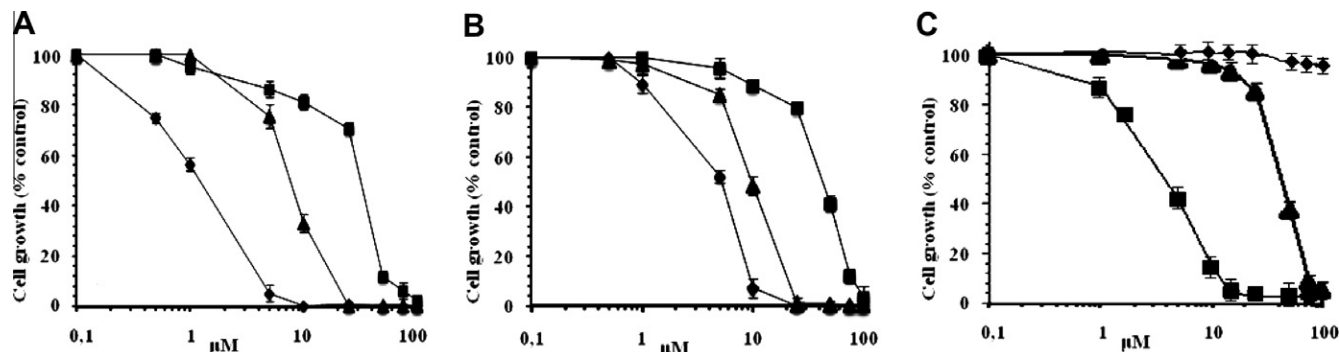


Figure 5. Dose–response curves obtained from M14 cells (A), A549 (B) and NIH3T3 normal fibroblasts (C) exposed to **VII** (\blacklozenge), **VIII** (\blacktriangle) and **IX** (\blacksquare) for 5 days. Points represent mean values \pm SD of three independent experiments.

satellite to allow the synthesis of new series of derivatives characterized by different lateral chains. These compounds can be regarded as a further class of G-quadruplex ligands providing proof of concept for the inhibition of telomerase in anticancer therapy. However, our interest is also focused on the interaction of these compounds with other type of biologically important quadruplex structures formed by human genetic regions as *c-myc*, *c-kit* and *bcl-2*.²⁶ At the moment, these investigations are in progress in our laboratories.

Supplementary data

Supplementary data associated with this article can be found, in the online version, at doi:10.1016/j.bmc.2011.08.062.

References and notes

- Huppert, J. L.; Subramanian, S. *Nucleic Acids Res.* **2005**, *33*, 2908.
- Wong, H. M.; Payet, L.; Huppert, J. L. *Curr. Opin. Mol. Ther.* **2009**, *11*, 146.
- Neidle, S. *FEBS J.* **2010**, *277*, 1118.
- Blackburn, E. H. *Nature* **1991**, *350*, 569.
- Blackburn, E. H. *Nature* **2000**, *408*, 53.
- Wang, Y.; Patel, D. J. *Structure* **1993**, *1*, 263.
- Parkinson, G. N.; Lee, M. P. H.; Neidle, S. *Nature* **2002**, *417*, 876.
- Luu, K. N.; Phan, A. T.; Kuryavyy, V.; Lacroix, L.; Patel, D. J. *J. Am. Chem. Soc.* **2006**, *128*, 9963.
- Ambrus, A.; Chen, D.; Dai, J.; Bialis, T.; Jones, R. A.; Yang, D. *Nucleic Acids Res.* **2006**, *34*, 2723.
- Zahler, A. M.; Williams, J. R.; Cech, T. R.; Prescott, D. M. *Nature* **1991**, *350*, 718.
- Kim, N. W.; Piatyszek, M. A.; Prowse, K. R.; Harley, C. B.; West, M. D.; Ho, P. L. C.; Coviello, G. M.; Wright, W. E.; Weinrich, S. L.; Shay, J. W. *Science* **1994**, *266*, 2011.
- Hahn, W. C.; Stewart, S. A.; Brooks, M. W.; York, S. G.; Eaton, E.; Kurachi, A.; Beijersbergen, R. L.; Knoll, J. H. M.; Meyerson, M.; Weinberg, R. A. *Nat. Med.* **1999**, *5*, 1164.
- Shay, J. W.; Wright, W. E. *Nat. Rev. Drug Disc.* **2006**, *5*, 577.
- Kelland, L. R. *Eur. J. Cancer* **2005**, *41*, 971.
- Neidle, S.; Parkinson, G. *Nat. Rev. Drug Disc.* **2002**, *1*, 383.
- Kelland, L. *Clin. Cancer Res.* **2007**, *13*, 4960.
- De Cian, A.; Lacroix, L.; Douarre, C.; Temine-Smaali, N.; Trentesaux, C.; Riou, J. F.; Mergny, J. L. *Biochimie* **2008**, *90*, 131.
- Sun, D.; Thompson, B.; Cathers, B. E.; Salazar, M.; Kerwin, S. M.; Trent, J. O.; Jenkins, T. C.; Neidle, S.; Hurley, L. H. *J. Med. Chem.* **1997**, *40*, 2113.
- Monchaud, D.; Teulade-Fichou, M. P. *Org. Biomol. Chem.* **2008**, *6*, 627.
- Fedoroff, O. Y.; Salazar, M.; Han, H.; Chemeris, V. V.; Kerwin, S. M.; Hurley, L. H. *Biochemistry* **1998**, *37*, 12367.
- Haider, S. M.; Parkinson, G. N.; Neidle, S. *J. Mol. Biol.* **2003**, *326*, 117.
- Gavathiotis, E.; Heald, R. A.; Stevens, M. F.; Searle, M. S. *J. Mol. Biol.* **2003**, *334*, 25.
- Campbell, N. H.; Parkinson, G. N.; Reszka, A. P.; Neidle, S. *J. Am. Chem. Soc.* **2008**, *130*, 6722.
- Parkinson, G. N.; Cuenca, F.; Neidle, S. *J. Mol. Biol.* **2008**, *381*, 1145.
- Campbell, N. H.; Patel, M.; Tofa, A. B.; Ghosh, R.; Parkinson, G. N.; Neidle, S. *Biochemistry* **2009**, *48*, 1675.
- Ou, T.-M.; Lu, Y.-J.; Tan, J.-H.; Huang, Z.-S.; Wong, K.-Y.; Gu, L.-Q. *ChemMedChem* **2008**, *3*, 690.
- Sissi, C.; Lucatello, L.; Paul Krapcho, A.; Maloney, D. J.; Boxer, M. B.; Camarasa, M. V.; Pezzoni, G.; Menta, E.; Palumbo, M. *Bioorg. Med. Chem.* **2007**, *15*, 555.
- Braña, M. F.; Castellano, J. M.; Moran, M.; Perez de Vega, M. J.; Romerdahl, C. R.; Qian, X. D.; Bousquet, P.; Emling, F.; Schlick, E.; Keilhauer, G. *Anti-Cancer Drug Des.* **1993**, *8*, 257.
- Cantor, C. R.; Warshaw, M. M.; Shapiro, H. *Biopolymers* **1970**, *9*, 1059.
- Arora, A.; Balasubramanian, C.; Kumar, N.; Agrawal, S.; Ojha, R. P.; Maiti, S. *FEBS J.* **2008**, *275*, 3971.
- Mergny, J. L.; Phan, A. T.; Lacroix, L. *FEBS Lett.* **1998**, *435*, 74.
- Mergny, J. L.; Lacroix, L. *Oligonucleotides* **2003**, *13*, 515.
- Pagnini, U.; De Martino, L.; Montagnaro, S.; Diodato, A.; Longo, M.; Pacelli, F.; Pisanelli, G.; Iovane, G. *Vet. Microbiol.* **2006**, *113*, 231.
- Kim, N. W.; Piatyszek, M. A.; Prowse, K. R.; Harley, C. B.; West, M. D.; Ho, P. L.; Coviello, G. M.; Wright, W. E.; Weinrich, S. L.; Shay, J. W. *Science* **1994**, *266*, 2011.
- Mosmann, T. *J. Immunol. Methods* **1983**, *65*, 55.
- Mi, N.; Seo, H. J.; Kim, Y.; Seo, S. H.; Rhim, H.; Cho, Y. S.; Cha, J. H.; Koh, H. Y.; Choo, H.; Pae, A. N. *Bioorg. Med. Chem.* **2007**, *15*, 365.
- Wang, Y. X.; Zhao, J.; Sun, X. Q.; Wang, C. J. *Chin. J. Org. Chem.* **2006**, *26*, 1066.
- Pagano, B.; Giancola, C. *Curr. Cancer Drug Targets* **2007**, *7*, 520.
- Lim, K. W.; Alberti, P.; Guédin, A.; Lacroix, L.; Riou, J.-F.; Royle, N. J.; Mergny, J.-L.; Phan, A. T. *Nucleic Acids Res.* **2009**, *37*, 6239.
- Jelesarov, I.; Bosshard, H. R. *J. Mol. Recognit.* **1999**, *12*, 3.
- Pagano, B.; Fotticchia, I.; De Tito, S.; Mattia, C. A.; Mayol, L.; Novellino, E.; Randazzo, A.; Giancola, C. *J. Nucleic Acids* **2010** doi:10.4061/2010/247137.
- Cosconati, S.; Marinelli, L.; Trotta, R.; Virno, A.; De Tito, S.; Romagnoli, R.; Pagano, B.; Limongelli, V.; Giancola, C.; Baraldi, P. G.; Mayol, L.; Novellino, E.; Randazzo, A. *J. Am. Chem. Soc.* **2010**, *132*, 6425.
- Pagano, B.; Mattia, C. A.; Giancola, C. *Int. J. Mol. Sci.* **2009**, *10*, 2935.
- Pagano, B.; Virno, A.; Mattia, C. A.; Mayol, L.; Randazzo, A.; Giancola, C. *Biochimie* **2008**, *90*, 1224.
- Martino, L.; Pagano, B.; Fotticchia, I.; Neidle, S.; Giancola, C. *J. Phys. Chem. B* **2009**, *113*, 14779.
- Martino, L.; Virno, A.; Pagano, B.; Virgilio, A.; Di Micco, S.; Galeone, A.; Giancola, C.; Bifulco, G.; Mayol, L.; Randazzo, A. *J. Am. Chem. Soc.* **2007**, *129*, 16048.
- Zhou, J.-M.; Zhu, X.-F.; Lu, Y.-J.; Deng, R.; Huang, Z.-S.; Mei, Y.-P.; Wang, Y.; Huang, W.-L.; Liu, Z.-C.; Gu, L.-Q.; Zeng, Y.-X. *Oncogene* **2006**, *25*, 503.
- Shalaby, T.; von Bueren, A. O.; Hürlimann, M.-L.; Fiaschetti, G.; Castelletti, D.; Masayuki, T.; Nagasawa, K.; Arcaro, A.; Jelesarov, I.; Shin-ya, K.; Grotzer, M. *Mol. Cancer Ther.* **2010**, *9*, 167.
- Sun, R. W.-Y.; Li, C. K.-L.; Ma, D.-L.; Yan, J. J.; Lok, C.-N.; Leung, C.-H.; Zhu, N.; Che, C.-M. *Chem. Eur. J.* **2010**, *16*, 3097.
- Bugelski, P. J.; Atif, U.; Molton, S.; Toeg, I.; Lord, P. G.; Morgan, D. G. *Pharm. Res.* **2000**, *17*, 1265.
- White, E. W.; Tanius, F.; Ismail, M. A.; Reszka, A. P.; Neidle, S.; Boykin, D. W.; Wilson, W. D. *Biophys. Chem.* **2007**, *126*, 140.
- Burger, A. M.; Dai, F.; Schultes, C. M.; Reszka, A. P.; Moore, M. J.; Double, J. A.; Neidle, S. *Cancer Res.* **2005**, *65*, 1489.
- Hampel, S. M.; Sidibe, A.; Gunaratnam, M.; Riou, J.-F.; Neidle, S. *Bioorg. Med. Chem. Lett.* **2010**, *20*, 6459.